Chemical Engineering Journal 164 (2010) 403–409

Contents lists available at ScienceDirect

Chemical Engineering Journal

journal homepage: www.elsevier.com/locate/cej

Markov chain modelling of fluidised bed granulation

Muammer Catak*, Nurşin Baş, Kevin Cronin, Dario Tellez-Medina, Edmond P. Byrne, John J. Fitzpatrick

Department of Chemical and Process Engineering, University College Cork, College Road, Cork, Ireland

ARTICLE INFO

Article history:
Received 7 September 2009
Received in revised form 3 February 2010
Accepted 9 February 2010

Keywords:
Granulation
Population balance modelling
Markov chains
Aggregation
Breakage

ABSTRACT

Fluidised bed granulation (FBG) is a particle size enlargement technique which is widely employed in industry. Modelling of FBG is important in order to understand, control and optimise the process. In literature, population balance modelling (PBM) which is based on population balance equations (PBEs) is a common tool to model the processing of these particulate systems. However, the solution of PBEs is not straightforward except for relatively simple cases. In this paper, Markov chain simulation is introduced in order to model and analyse the particle size enlargement process in fluidised bed granulation where aggregation and breakage occur simultaneously. For the study, the size enlargement process of granules based on glass beads is examined. 10 g PEG (poly ethylene glycol) with 60% concentration is used as the binder for a 200 g batch. The results show that Markov chains are an efficient tool to model the granulation process. Particle size enlargement and the shape of particle size distributions during the granulation process have been estimated within acceptable errors.

1. Introduction

Fluidised bed granulation (FBG) is a particle size enlargement technique especially prevalent in industries concerned with pharmaceuticals, detergents, fertilisers, and food. Common reasons for granulation are to obtain a narrow band particle size distribution, to improve flow properties and to avoid cake formation during storage. In FBG, a liquid binder solution is injected into the bed usually by a nozzle. There are three different types of FBG according to spray method employed that are top spray, bottom spray and tangential spray. The purpose of the binder is to produce wet and sticky particle surfaces and hence promote agglomeration when inter-particle collisions occur. Whether a collision successfully results in granulation is determined by the granulation mechanism which in turn depends on particle and bed properties.

Modelling of such processes is required for understanding the entire process and for process design and optimisation. Population balance modelling (PBM) which is mostly based on the law of mass conservation is widely used to model such particulate systems. A mathematical function of the distribution of a certain property such as mass, diameter, and temperature of the particles is found by using population balance equations (PBEs). PBM is quite powerful in analyzing the dynamics of the process, however, the structure of PBEs is complex due to the intrinsic partial integro-differential equations and hence analytical solutions may not be possible except for simple cases. There have been many research studies dealing with aggregation and breakage processes using population balance equations [1–8].

Stochastic models which can be based on Markov chain theory is a very valuable tool because of its simplicity and flexibility. Although, the Markov theory has been used in many fields such as astronomy, biology, computer science, communications, forecast, game theory and radio engineering after Andrei Andreevich Markov (1856–1922) released his work [9], it has been used less than its deserving value in chemical engineering. Even it can be stated that it is still unknown/unapplied in chemical engineering. There is only one book which was published in 1998 on application of Markov chains in chemical engineering [10]. A list of applications of Markov chains in chemical engineering and powder technology is as follows: particle flow in fluidised bed [11–13], particle mixing [14–16], and particle breakage [17–19].

In this paper the Markov chain method is used to model and analyse particle size enlargement in fluidised bed granulation where aggregation and breakage occur simultaneously.

2. Theory

2.1. Markov chains

A Markov process is defined by a transition matrix **P**, a state vector $\mathbf{a}(t)$ and a transition time step τ. The transition matrix **P** has entries p_{ij} which represents transition probabilities from state i to

* Corresponding author. Tel.: +353 873231172.
E-mail address: muammer.catak@gmail.com (M. Catak).

1385-8947/$ – see front matter © 2010 Elsevier B.V. All rights reserved.
doi:10.1016/j.cej.2010.02.022

state j at each time step. On this basis, the transition matrix $\mathbf{P}$ is given by $n \times n$ matrix as follows [20]:

$$\mathbf{P} = \begin{bmatrix} p_{11} & p_{12} & \dots & p_{1n} \\ p_{21} & p_{22} & \dots & p_{2n} \\ \dots & \dots & \dots & \dots \\ p_{n1} & p_{n2} & \dots & p_{nn} \end{bmatrix}_{n\times n}$$

$$a_i(t+1) = \sum_{j=1}^{n} p_{ji} a_j(t)$$

$$[a_1(1),\ a_2(1), \dots,\ a_n(1)] = [a_1(0),\ a_2(0), \dots,\ a_n(0)] \times \begin{bmatrix} p_{11} & p_{12} & \dots & p_{1n} \\ p_{21} & p_{22} & \dots & p_{2n} \\ \dots & \dots & \dots & \dots \\ p_{n1} & p_{n2} & \dots & p_{nn} \end{bmatrix}$$

$$\mathbf{a}(t+m) = \mathbf{a}(t)\mathbf{P}^m$$

The vector $\mathbf{a}(t)$with components $a_1(t), a_2(t), \dots, a_n(t)$ is called the state probability distribution vector of the system at time t. If the probability for an entity currently in the state j at time t is denoted by $a_j(t)$ then the state probability distribution of state i for the next time step, $a_i(t+1)$is given by the sum of product of all probabilities. This is formulated as follows:

$$a_i(t+1) = \sum_{j=1}^{n} p_{ji} a_j(t) \tag{1}$$

The general form of Eq. (1) for time-homogeneous and nonhomogeneous transition matrices $\mathbf{P}$ for different time steps can be given by the following equations, respectively;

$$\mathbf{a}(t+m) = \mathbf{a}(t)\mathbf{P}^m \tag{2.a}$$

$$\mathbf{a}(t+1) = \mathbf{a}(t)\mathbf{P}(t) \tag{2.b}$$

The transition matrix $\mathbf{P}$ is built up by using the breakage and aggregation functions which come from population balance modelling terminology. Such Markov chain modelling is based on mass balance equations as with PBM. From this perspective, it can be viewed as a possible discrete solution mechanism of PBM. Moreover, it offers the possibility of replacing PBM in some aspects of granulation analysis, since it has equal efficiency but is less time consuming.

2.2. Population balance modelling

The general continuous form of the population balance equation for modelling aggregation and breakage processes that occur simultaneously can be given as follows [21]:

$$\frac{\partial V(x,t)}{dt} = \int_x^\infty q(x,y)b(y)V(y,t)dy - b(x)V(x,t) + \frac{1}{2}\int_0^x \alpha(x-\varepsilon,\varepsilon)V(x-\varepsilon,t)V(\varepsilon,t)d\varepsilon - V(\varepsilon,t)\int_0^\infty \alpha(x,\varepsilon)V(\varepsilon,t)d\varepsilon \tag{3}$$

where x is the particle volume, $V(x,t)$ is the volume fraction density function of particles of volume x at time t, $q(x,y)$ is called fragment particle size distribution, and it is the probability distribution of particles of size x being formed from a break-up process of particles of diameter y. The area under the curve of $q(x,y)$ must equal 1 due to the law of mass conservation. $b(x)$ is the breakage frequency. The function which is obtained by multiplication of $b(x)$ and $q(x,y)$ is called the breakage kernel. $a(x,\varepsilon)$ is aggregation kernel which indicates production rate of particle of volume $x+\varepsilon$ from particles of volume of x and volume of ε. It is defined as

$$\alpha(x,\varepsilon) = \alpha_0 g(x,\varepsilon) \tag{4}$$

a_0 is the aggregation frequency which depends on process parameters and is mostly constant for a particular process parameters, $g(x,\varepsilon)$ is the aggregation probability distribution. The first line of Eq. (3) represents the breakage and the second line comprises the aggregation.

In the literature it is common to assume that the breakage frequency is proportional to volume of the particle as [22]

$$b(x) = kx \tag{5}$$

where k is an arbitrary constant and x is particle volume. Accordingly, the discrete breakage frequency can be written as

$$b_i = kx_i \equiv kl_i^3 \tag{6}$$

where x_i and l_i are representative volume size and diameter of interval i, respectively.

The fragment particle size distribution should be chosen bearing in mind process parameters. Berthiaux et al. [18] used the following formulae for particle breakage in which the particle can transit only into neighbouring intervals as

$$q_{jm} = \frac{x_m}{x_{j-1}^R + x_m^R} \tag{7}$$

where $1 < R < 2$. If the restriction on only permitting passage to adjacent states is removed, then the distribution function in Eq. (7) can be generalized as

$$q_{ij} = \frac{x_j^R}{x_1^R + x_2^R + \dots + x_j^R + \dots + x_{i-1}^R} = \frac{x_j^R}{\sum_{k=1}^{i-1} x_k^R} \quad \text{for all } i \tag{8}$$

and Eq. (8) will be subsequently used. Tan et al. [23] described aggregation kernel in two functions; the product of a size independent term α_0 and a term that is a function of the agglomerating particle sizes l_i and l_j, respectively.

$$\alpha_{ij} = \alpha_0 (l_i + l_j)^2 \sqrt{\frac{1}{l_i^3} + \frac{1}{l_j^3}} \tag{9}$$

Specifically l_i and l_j are the representative particle diameter in the size intervals i and j, respectively. A physical interpretation of Eq. (9) is that the more the two colliding particles differ in size, the more likely they are to aggregate; conversely equal sized particles are less likely to agglomerate. A visual implementation of Eq. (9) can be seen in Fig. 1.

Eq. (9) can be written to obtain a discrete probability distribution as

$$\alpha_{ij} = \alpha_0 \frac{(l_i + l_j)^2 \sqrt{(1/l_i^3) + (1/l_j^3)}}{\sum_{j=1}^{n} (l_i + l_j)^2 \sqrt{(1/l_i^3) + (1/l_j^3)}} \tag{10}$$

Then, the probability of particles in ith interval may transit to interval j is written as

$$g_{ij} = \begin{cases} \dfrac{(l_i + l_{j-i})^2 \sqrt{(1/l_i^3) + (1/l_{j-i}^3)}}{\sum_{j=i+1}^{2n} (l_i + l_{j-i})^2 \sqrt{(1/l_i^3) + (1/l_{j-i}^3)}} & \text{if } i \le n \\ 0 & \text{else} \end{cases} \tag{11}$$

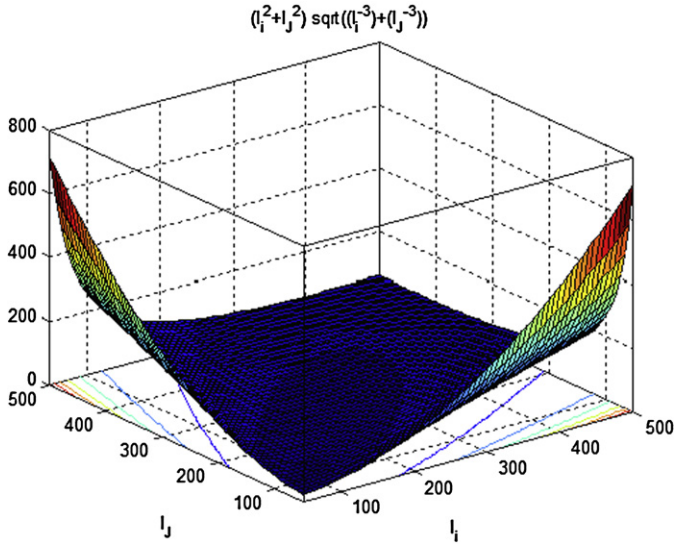

Fig. 1. Graphical representation of Eq. (9).

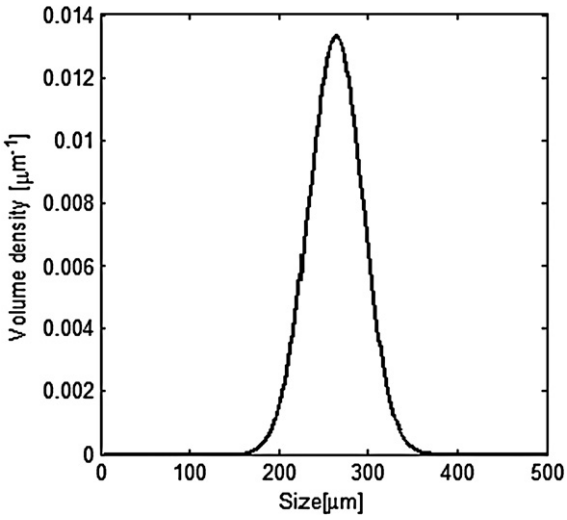

Fig. 2. Initial particle size distribution of glass beads.

2.3. Markov solution

In this section the PBE in Eq. (3) is rewritten to conform with the Markov algorithm. Assuming the initial size range is divided into n state spaces which are enough to represent the process, thus the discrete size domain is obtained. If the maximum particle size which can aggregate in the system is represented by the nth interval, then the number of the intervals will be $2n$ using a uniform discretization procedure. On this basis, breakage and aggregation functions must be converted into a discrete form. A particle in any interval can go to a higher interval by aggregating, or can go down to a lower interval as a result of a breakage, or it can stay in the same interval after a transition time step. The transition matrix can thus be divided into three parts as regards the modelling algorithm.

- Diagonal entries contain the probability that the particle can stay in the same interval after a transition time step. If α_i and b_i are the aggregation and breakage frequencies of the ith interval, then the probability that the particle stays in the same interval is

$$p_{ii} = (1 - \alpha_i - b_i) \tag{12}$$

- Upper diagonal entries represent the aggregation process. The probability that the particle will go to size interval j from size interval i can be written as

$$p_{ij} = \alpha_i g_{ij} \quad \text{if} j > i \tag{13}$$

- Entries below the diagonal comprise the breakage process. The probability that the particle goes to interval j from the interval i due to a breakage can be written as

$$p_{ij} = b_i q_{ij} \quad \text{if} j < i \tag{14}$$

The transition matrix $p_{n\times n}$ combines the entries which are described in Eqs. (12)–(14).

$$\mathbf{P} = \begin{cases} p_{ii} = (1 - \alpha_i - b_i) & \\ p_{ij} = \alpha_i g_{ij} & \text{if} j > i (\text{aggregation}) \\ p_{ij} = b_i q_{ij} & \text{if} j < i (\text{breakage}) \end{cases} \tag{15}$$

3. Materials and methods

3.1. Experiments

For this study, the size enlargement process of glass beads is examined. These consist of spherical particles whose diameter can be represented by the normal distribution with mean $\mu = 263$ μm and standard deviation $\sigma = 30$ μm illustrated in Fig. 2. Average density of the beads is 2365 kg/m^3.

10 g PEG 1500 (poly ethylene glycol) at 60% aqueous concentration is used as the binder for a 200 g batch of beads. Specifications of binder are listed in Table 1.

During the experiments the overall air flow rate was 0.65 m^3/min. Density of the air is taken to be 1.2 kg/m^3 while dynamic viscosity is 1.85×10^{-5} Pa s.

The experiments reported here were carried out using the Mini-Airpro fluidised bed granulator (Pro-C-epT Mini-AirPro, Belgium). A simplified schematic diagram for the experimental setup is given in Fig. 3. For all experiments, the bottom spray nozzle was located half way up the Würster column. The upper half of the column is denoted the spray zone where most particle and binder droplet interaction occurs.

The experimental conditions that were used are shown in Table 2.

The granules were produced according to following experimental procedure:

- The fluidised bed was heated by the air to obtain the designated bed temperature. This process took 8 min.
- The fluidised air was stopped and 200 g of glass beads placed into the rig.
- The bed was fluidised for a few minutes at a low air flow rate (around 0.4 m^3/min) until the bed temperature stabilised to the designated temperature.

Table 1
Specifications of binder solution.

Density at 18 °C	1009 kg/m^3
Dynamic viscosity at 18 °C	0.215 Pas
Surface tension at 18 °C	5.34×10^{-2} N/m
Water diffusion coefficient in air at 35 °C	2.6×10^{-5} m^2/s
Water specific gas constant	461.889 J/kg K

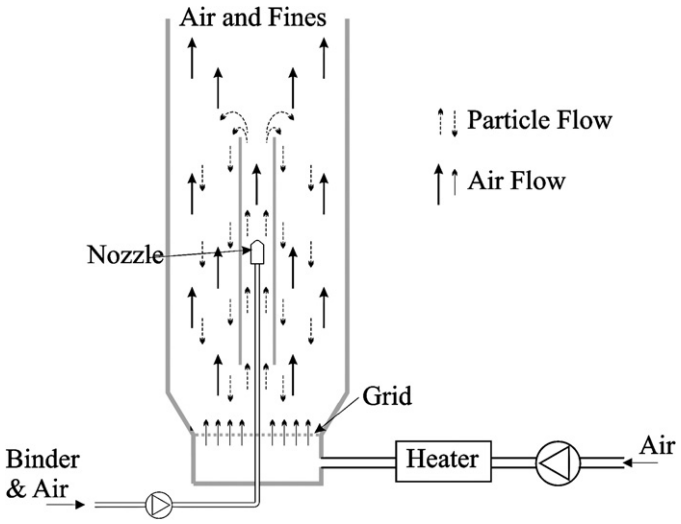

Fig. 3. Fluidised bed granulator, Würster type.

- The nozzle was inserted and the air flow rate increased to designated flow rate of 0.65 m^3/min, then the binder injection commenced.
- Every 2.5 min small amount of sample was taken.
- After 25 min binder injection was stopped to cease granulation.
- Drying of the granules for the final last minute.

During the process about 3 g samples were taken by sample probe at an interval of 2.5 min. To check the reliability of the samples, the process was stopped at the corresponding time and the particle size of the whole bed measured. It was observed that samples can represent the whole particles with an acceptable error at each time. The Camsizer (Retsch Technology, Germany) is based on digital image processing with a two camera system which is suitable for solids in the range from 30 μm to 30 mm and was used to measure the particle size distribution.

3.2. Model implementation

The Matlab software package is used for the calculations. Granule size can be discretized using a uniform or geometric ratio scheme; for this paper the geometric method is used. The whole size range from 138 μm to 5500 μm was divided into 40 intervals with a consecutive diameter ratio of 1.1. Then the representative size of each interval is calculated using geometric mean of ends of the intervals such as

$$l_i = \sqrt{d_i d_{i-1}} \tag{16}$$

Table 2
Experimental setup.

Batch size	200 g
Inlet-air pressure	6 bar
Inlet-air flow	0.65 m^3/min
Inlet-air temperature	35 °C
Outlet-air temperature	31.2 °C
Near-product air temperature	31.6 °C
Nozzle-air pressure	2.5 bar
Liquid addition rate	0.4 g/min
Total amount of liquid	10 g
Time required to add total amount of liquid	25 min
Extra time to dry product	1 min
Total processing time	34 min

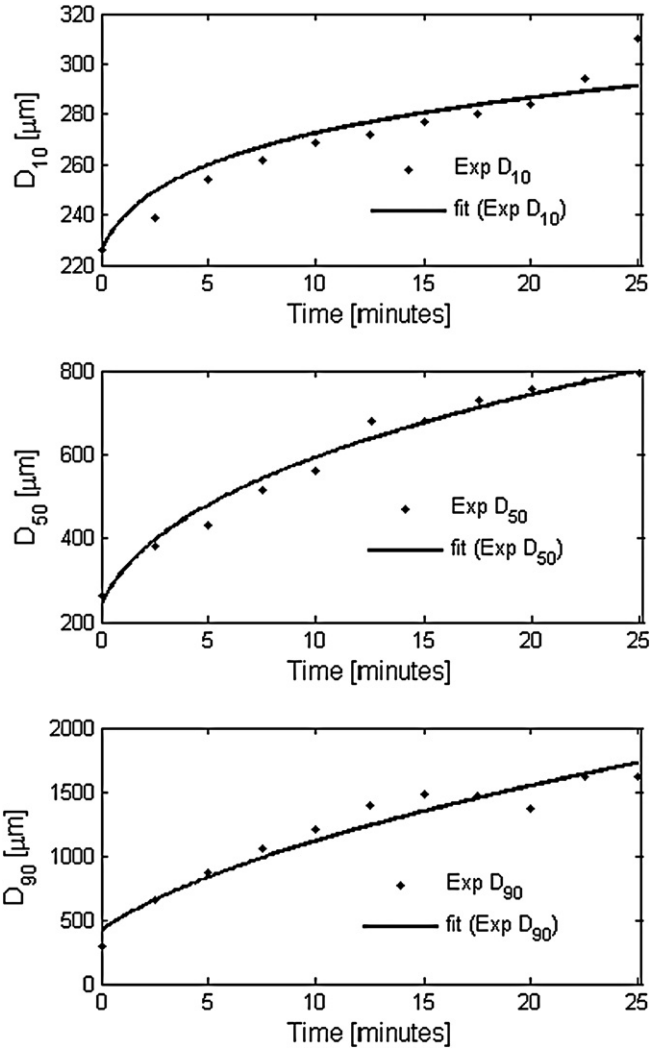

Fig. 4. D_{10}, D_{50}, and D_{90} evolutions of granulation process.

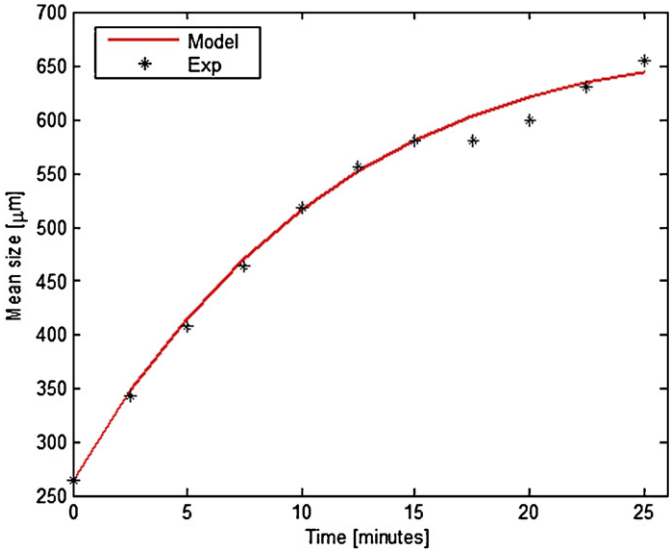

Fig. 5. Comparisons of predicted and experimental mean sizes.

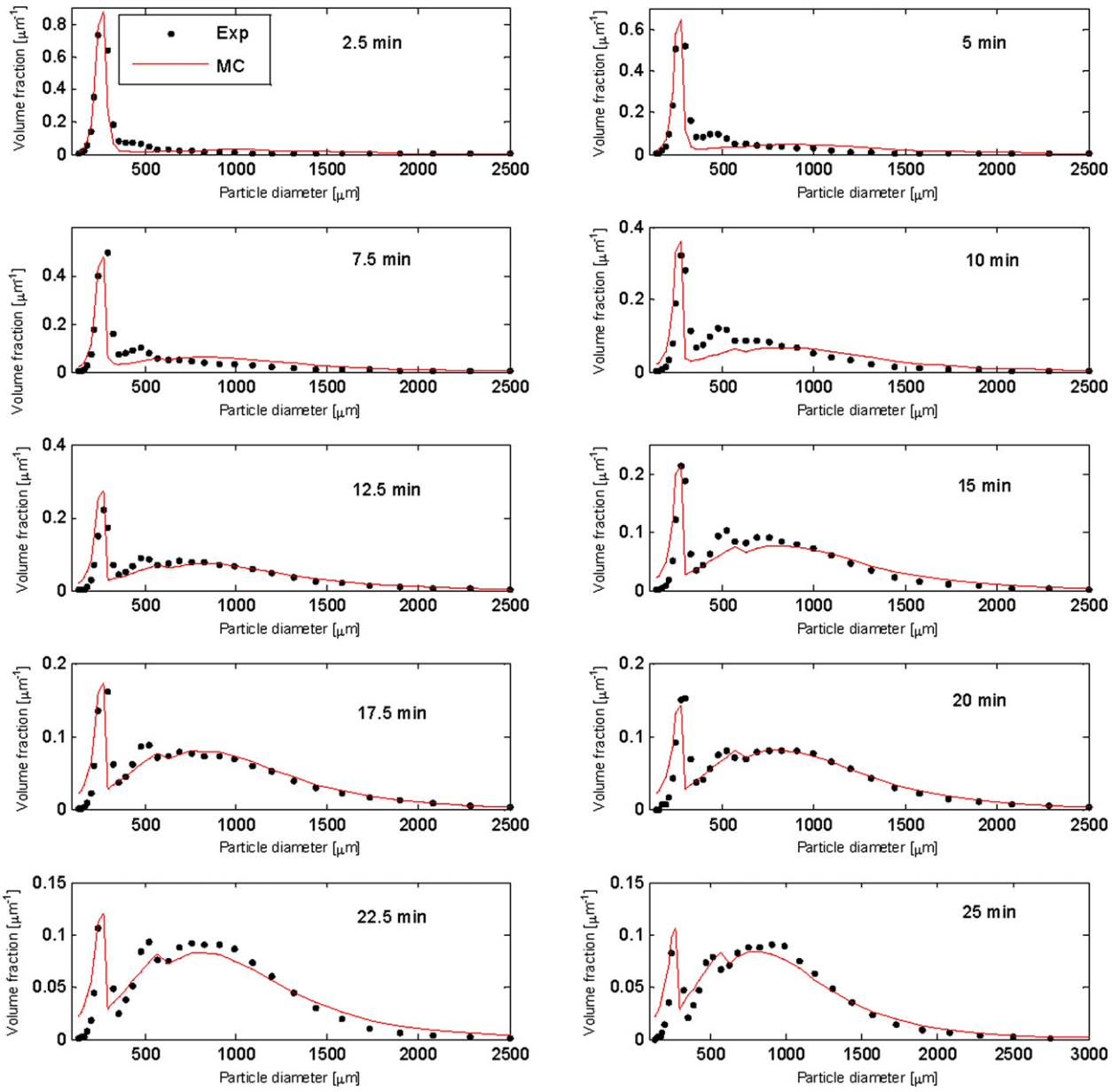

Fig. 6. Particle size distributions obtained from the model and experiments for various times.

where d_i and d_{i-1} are upper and lower size ends of ith interval. The magnitudes of the constant aggregation frequency, α_0, the constant breakage frequency rate, k and the constant in the fragment particle size distribution, R must be chosen from analysis of the experimental data. Initially, these parameters were obtained by minimizing the error between predicted and experimental D_{10}, D_{50} and D_{90} of granule size versus time (see Fig. 4). For the validation of the Markov model, an independent set of experimental data obtained by following same experimental procedure was used. Using the maximum likelihood approach, which aims to achieve the minimum squared error between the model and the experimental measurements of the mean size, the optimum α_0, k and R values were obtained as

$$\text{find the optimum values of } \{\alpha_0, k, R\} \text{ for min} \left\{ \sum_{i=1}^{n} (E_i - M_i)^2 \right\}$$

The experimentally measured particle size distribution exhibited a bimodal characteristic. From a statistical analysis of the results, it was found that particles smaller than 350 μm had an aggregation frequency that was a third of larger sized particles. Hence for this data, the constant aggregation frequency is taken as $\alpha_0 = 6 \times 10^{-3}\ s^{-1}$ for particles those are bigger than 350 μm and taken as $\alpha_0 = 2 \times 10^{-3}\ s^{-1}$ for particles those are smaller than 350 μm, the constant breakage frequency rate is taken as $k = 7.96 \times 10^{-12}\ mm^{-3}\ s^{-1}$ and the constant R in the fragment particle size distribution is chosen as 1.05.

The Markov chain method requires an initial state vector $\mathbf{a}(0)$, a transition matrix $\mathbf{P}_{40\times40}$ and a transition time step τ to be selected. The initial vector comes from the discretization of the probability density function for size that is illustrated in Fig. 2. The entries in the transition matrix are found from the method explained in Section 2.2. Determination of the magnitude of the time step, τ is more arbitrary. Since the aggregation frequency α_0 is constant, then the model is relatively insensitive to the time step size (once it is suf-

ficiently small). For this work, τ is arbitrarily selected as 1 s for the illustration of the process.

4. Results and discussions

Comparisons between the predicted mean sizes and the experimental mean sizes are displayed in Fig. 5. Although, the Markov model overestimates the mean size at 17 and 20 min; and underestimates at 25 min, the overall agreement is very good in the process.

The particle size distributions obtained from the model and experiments for various times are shown in Fig. 6. The particle size has uni-modal distribution at the start (see Fig. 2). At later stages of the process, the size distribution might be viewed as having a tri-modal shape with the first peak between 100 μm and 350 μm, the second peak located between 350 μm and 600 μm and the third peak beyond 600 μm. These peaks are more clearly visible especially after 10 min of the process. On the other hand, the second peak is not very pronounced and to avoid an excessively complex model, the actual particle size distribution is assumed to be bimodal. The model captures the bimodal shape of the particle size distribution and matches the experimental results. Qualitatively it can be noticed that the agreement between the model and the experiment is better for large and small particles than intermediate sized particles. The selected aggregation and breakage functions might cause that slight disagreement for medium size particles. In addition statistical analysis of the results was carried out. According to Kolmogorov-Smirnov test [24], the agreement between the model and the experimental results is not less than 90% over the process. If the aggregation process is significantly dominant over the breakage process, then the whole particle size enlargement process might be represented just using aggregation functions. However, in this system, breakage also has important role in determining the particle size distribution of the glass beads. Therefore both breakage and aggregation functions must be simultaneously used in modelling.

5. Conclusions

One dimensional population balance modelling based on size property has been applied to model the particle size enlargement process of glass beads where both aggregation and breakage occur simultaneously. In addition, the Markov chain method has been used to solve the PBM. The results show that the Markov chain method, which is based on population balance concepts, works well for the particle size enlargement process of glass beads of this study. For future work, a better agreement between model and experiment might be achieved taking into account the three-modal shape and increasing the number of the states of the system. Also different fragment size particle distributions and/or different aggregation probability functions might be used, and the results compared to find the best fitted functions for the bottom spray Würster type fluidised bed granulation.

Nomenclature

$\mathbf{P}$	Markovian transition matrix
$\mathbf{a}(t)$	state probability vector
τ	tratatensition time step (s)
x	particle volume (mm^3)
$V(x, t)$	volume fraction density function of particles of volume x at time t
$q(x, y)$	fragment particle size distribution
$b(x)$	breakage frequency (s^{-1})
$a(x, \varepsilon)$	aggregation kernel (s^{-1})
a_0	aggregation frequency (s^{-1})
$g(x, \varepsilon)$	aggregation probability distribution
x_i	representative volume of interval i (mm^3)
l_i	representative diameter of interval i (mm)
t	time (s)

Acknowledgements

This publication has emanated from research conducted with the financial support of Science Foundation Ireland. Authors N. Bas, E. Byrne and J.J. Fitzpatrick would like to acknowledge the National Development Plan, through the Food Institutional Research Measure, administered by the Department of Agriculture, Fisheries and Food, Ireland for providing funding for this work.

References

[1] S. Kumar, D. Ramkrishna, On the solution of population balance equations by discretization-I: a fixed pivot technique, Chemical Engineering Science 51 (1996) 1311–1332.
[2] R. Diemer, J. Olson, A moment methodology for coagulation and breakage problems: Part 1. Analytical solution of the steady-state population balance, Chemical Engineering Science 57 (2002) 2193–2209.
[3] D.L. Marchisio, J.T. Pikturna, R.O. Fox, D.R. Vigil, A.A. Barresi, Quadrature method of moments for population-balance equations, AIChE Journal 49 (2003) 1266–1276.
[4] C. Immanuel, F. Doyle-III, Solution technique for a multi-dimensional population balance model describing granulation processes, Powder Technology 156 (2005) 213–225.
[5] N.K. Nere, D. Ramkrishna, Evolution of drop size distributions in fully developed turbulent pipe flow of a liquid–liquid dispersion by breakage, Industrial & Engineering Chemistry Research 44 (2005) 1187–1193.
[6] M. Kostoglou, A. Karabelas, On the breakage of liquid–liquid dispersions in turbulent pipe flow: spatial patterns of breakage intensity, Industrial & Engineering Chemistry Research 46 (2007) 8220–8228.
[7] J.M.-H. Poon, C.D. Immanuel, F.J. Doyle III, J.D. Litster, A three dimensional population balance model of granulation with a mechanistic representation of the nucleation and aggregation phenomena, Chemical Engineering Science 63 (2008) 1315–1329.
[8] N. Bas, M. Catak, N. Zumaeta, J.J. Fitzpatrick, K. Cronin, E.P. Byrne, Population balance modelling of protein precipitates exhibiting turbulent flow through a circular pipe, Chemical Engineering Science 64 (2009) 4051–4059.
[9] A.A. Markov, Extension of the law of large numbers to dependent events, Bulletin of the Society of the Physics Mathematics 15 (1906) 155–156.
[10] A. Tamir, Applications of Markov Chains in Chemical Engineering, Elsevier, Amsterdam, The Netherlands, 1998.
[11] R. Fox, L. Fan, Stochastic analysis of axial solids mixing in a fluidised bed, in: Proceedings of the 1st World Congress on Particle Technology Part 3, Nurnberg, Germany, 1986, pp. 581–595.
[12] H. Dehling, A. Hoffmann, H. Stuut, Stochastic models for transport in a fluidized bed, SIAM Journal of Applied Mathematics 60 (1999) 337–358.
[13] A.T. Harris, R.B. Thorpe, J.F. Davidson, Stochastic modelling of the particle residence time distribution in circulating fluidised bed risers, Chemical Engineering Science 57 (2002) 4779–4796.
[14] M. Aoun-Habbache, M. Aoun, H. Berthiaux, V. Mizonov, An experimental method and a Markov chain model to describe axial and radial mixing in a hoop mixer, Powder Technology 128 (2002) 159–167.
[15] H. Berthiaux, K. Marikh, V. Mizonov, D. Ponomarev, E. Barantzeva, Modelling continues powder mixing by means of the theory of Markov chains, Particulate Science and Technology 22 (2004) 379–389.
[16] D. Ponomarev, V. Mizonov, C. Gatumel, H. Berthiaux, E. Barantzeva, Markov-chain modelling and experimental investigation of powder-mixing kinetics in static revolving mixers, Chemical Engineering and Processing 48 (2009) 828–836.
[17] H. Berthiaux, Analysis of grinding processes by Markov chains, Chemical Engineering Science 55 (2000) 4117–4127.
[18] H. Berthiaux, V. Mizonov, V. Zhukov, Application of the theory of Markov chains to model different processes in particle technology, Powder Technology 157 (2005) 128–137.
[19] J. Chakraborty, D. Ramkrishna, Identification of Markov matrices of milling models, Industrial & Engineering Chemistry Research 48 (2009) 9763–9771.
[20] L. Farina, S. Rinaldi, Positive Linear Systems: Theory and Applications, Wiley, New York, 2000.
[21] D. Ramkrishna, Population Balances Theory and applications to Particulate Systems in Engineering, Academic Press, USA, 2000.

[22] H.S. Tan, A.D. Salman, M.J. Hounslow, Kinetics of fluidised bed melt granulationV: Simultaneous modelling of aggregation and breakage, Chemical Engineering Science 60 (2005) 3847–3866.
[23] H.S. Tan, M.J.V. Goldschmidt, R. Boerefijn, M.J. Hounslow, A.D. Salman, J.A.M. Kuipers, Building population balance model for fluidized bed melt granulation: lessons from kinetic theory of granular flow, Powder Technology 142 (2004) 103–109.
[24] F.J. Massey Jr., The Kolmogorov–Smirnov test for goodness of fit, Journal of the American Statistical Association 46 (253) (1951) 68–78.